EVLA Memo #165
The Impact of the New Thermal Gap Receiver Assembly on the Sensitivity of the EVLA at L-Band (1–2 GHz)

E. Momjian and R. Perley (NRAO)
and
R. Hayward

Original release date: November 16, 2012
Updated: December 11, 2014*

Abstract

We present sensitivity measurements of the EVLA at L-band between 1 and 2 GHz to assess the impact of the receivers with the new thermal gap assembly. Our on-the-sky test results are consistent with lab measurements, and show that the sensitivity improves by an average value of ∼7% in the frequency range 1–1.55 GHz, and degrades by an average value of ∼3% in the frequency range 1.55–2 GHz. The sensitivity improvement at the lower half of L-band will particularly be valuable for the study of various spectral line transitions that can be observed in this frequency range.

1 Introduction

In early 2012, a new thermal gap assembly was implemented on the L-band receiver system of the EVLA. Lab measurements showed clear improvement in the sensitivity below 1.6 GHz and above 1.95 GHz and a small degradation between 1.6 and 1.95 GHz, in both the RCP and LCP. Figure 1 shows a comparison of the receiver temperature between the old (*red*) and the new (*blue*) thermal gap assemblies of the first L-band receiver that underwent the modification. Upon completion of the lab tests, this receiver was installed on antenna ea05 in March 2012.

To assess the improvement in the sensitivity due to the new thermal gap assembly of the L-band receivers in astronomical observations, we have carried out various on-the-sky tests as soon as antenna ea05 was equipped with the modified receiver. However, the initial observations did not result in any useful data due to severe RFI, both internal and external. Successful observations were finally carried out when the array was in the most extended, A-configuration. At this time, we also had a total of three antennas that were equipped with the new thermal gap assembly L-band receivers.

2 Observations

The EVLA A-configuration observations at L-band were carried out on October 13, 2012, for a total of 0.5 hours. The calibrator source 3C48 (J0137+3309) and a field devoid of strong contin-

*This memo has been updated to include an appendix that describes the differences between the old and new thermal gap assemblies of the EVLA L-band and C-band receivers. Moreover, a paragraph and a figure have been added to the Results and Discussion section (§4) to explain the sensitivity trend seen between 1.6 and 1.8 GHz.

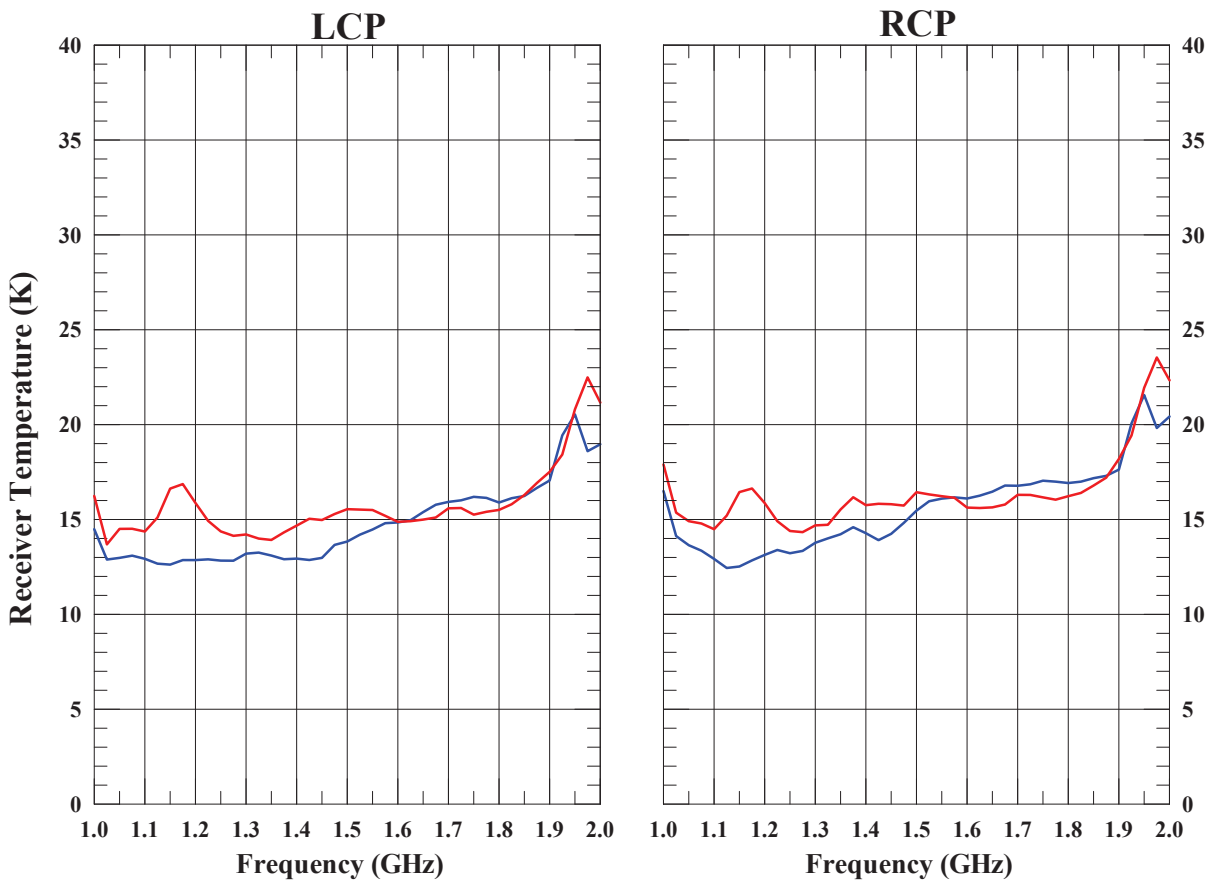

Figure 1: Lab measurements of the receiver temperature of an EVLA L-band receiver with the old (*red*) and new (*blue*) thermal gap assembly. The left-hand side plot is of the LCP, and the right-hand side plot is of the RCP. This receiver was later installed on antenna ea05.

uum sources (hereafter "blank field") were observed in this session. The WIDAR correlator was configured to deliver 16 adjacent sub-bands, each with 64 MHz bandwidth, 256 spectral channels, and dual polarization (RR and LL) products. The resulting spectral resolution was 250 kHz. The correlator integration time was set to 1 second.

3 Data Reduction and Analysis

Data reduction and analysis were carried out in AIPS. Upon loading the data, antennas that did not have the EVLA-compliant L-band receivers were edited out; see the EVLA Memo #152 (Momjian & Perley 2011) for a detailed discussion on the sensitivity of the EVLA-compliant L-band receivers. The flux density scale was set using the Baars et al. 1977 coefficients for 3C48. After applying a priori flagging and excising integrations affected by interference, antenna based delay, complex gain and bandpass calibration solutions were obtained using the data of the calibrator source 3C48 for each sub-band and polarization product (i.e., RR and LL) separately. These solutions were then applied on the visibilities of the blank field, and spectra were generated to visually inspect its data in order to further ensure the exclusion of spectral channels that were affected by RFI from subsequent analysis.

Using the AIPS task UVHGM, the RMS noise values for Stokes I were measured by fitting

Gaussian profiles on the histogram distributions of the blank field's real part of the visibilities. For this, we used channels from each sub-band that were not visibly contaminated by RFI. A 3-channel Hanning-smoothing was applied on the spectra in all the data reduction and analysis steps to reduce the Gibbs ringing phenomenon introduced by strong RFI features at various L-band frequencies.

As noted earlier, only three of the antennas in the data set, namely ea02, ea05, and ea26, were equipped with the L-band receivers that have the new thermal gap assembly. The sensitivity measurements reported in this memo are based on the average values of the baselines among these three EVLA antennas. For comparison, sensitivity measurements were also obtained using the average values of the baselines among three other antennas with comparable baseline lengths to those noted above.

Multiple background continuum sources in the blank field contribute a total of $S \sim 35$ mJy to our measurements, as determined by imaging one of the sub-bands. A correction was made to account for these background sources as follows:

$$\mathrm{RMS} = \sqrt{(\mathrm{RMS}_h)^2 - (S)^2}, \tag{1}$$

where RMS_h is the noise values obtained through the histogram fittings.

The corrected RMS noise values were then converted to System Equivalent Flux Densities (SEFDs) using the following equation:

$$\mathrm{RMS\ (Jy)} = \frac{1}{2\eta_c\kappa_{hs}} \frac{\mathrm{SEFD\ (Jy)}}{\sqrt{\beta\tau}}, \tag{2}$$

where β is the spectral channel width in Hz and τ is the correlator integration time in seconds. η_c is the WIDAR correlator efficiency, and it is assumed to be 0.93 for the mode used in these observations, and κ_{hs} is the improvement in the signal-to-noise due to the application of the Hanning-smoothing, which is 1.633[1] for a 3-channel Hanning-smoothing.

4 Results and Discussion

Figure 2 shows the SEFD values in the EVLA L-band frequency range $1 - 2$ GHz. The blue curve represents the average SEFD of the baselines among the three antennas that have the L-band receivers with the new thermal gap assembly (ea02, ea05, and ea26). The red curve represents the average SEFD of the baselines among three other antennas that have the old thermal gap assembly and which have comparable baseline lengths to the antennas used in making the measurements reflected by the blue curve. The results show a clear improvement in the sensitivity below 1550 MHz due to the new thermal gap assembly of the L-band receivers, and a slight sensitivity degradation above 1550 MHz.

Figure 3 shows the percentage change in the SEFD due to the new thermal gap assembly relative to the old thermal gap assembly. Positive values reflect lower SEFDs (i.e., improved sensitivity) due to the new thermal gap design. We note that at L-band the receiver temperature is about 50% of the system temperature. Therefore, the percentage improvement in the sensitivity would be about half of the percentage improvement seen in the receiver temperature (Figure 1). This is indeed the case in the on-the-sky test results.

As seen in Figure 3, the sensitivity has improved by an average value of $\sim$7% in the frequency range $1 - 1.55$ GHz. The peak sensitivity improvement is at 1150 MHz and it is by up to $\sim$13%. This is in excellent agreement with the lab measurements (Figure 1) that show a peak in the receiver temperature of the old thermal gap assembly around 1150 MHz. This feature is not seen in the receiver temperature of the new thermal gap assembly, and hence the largest improvement in

[1]The improvement in signal-to-noise due to a 3-channel Hanning-smoothing is $1/\sqrt{0.25^2 + 0.5^2 + 0.25^2}$=1.633

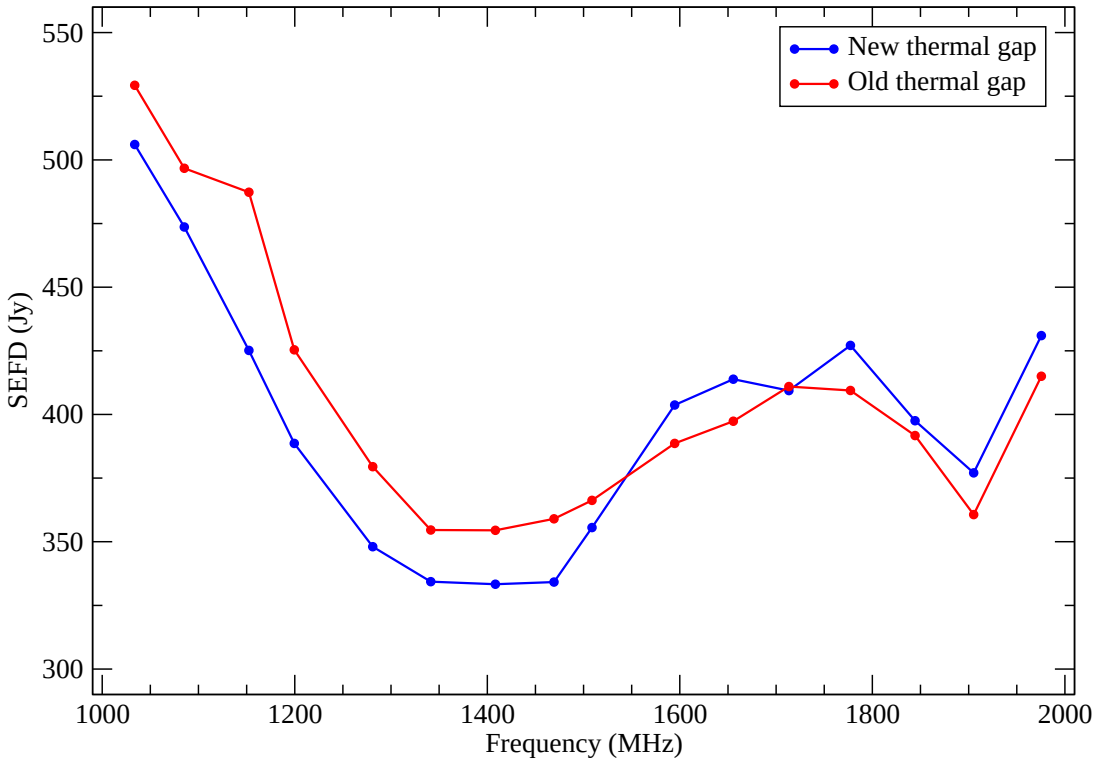

Figure 2: The SEFD values in the EVLA L-band frequency range $1 - 2$ GHz. The blue curve represents the average SEFD of the baselines among the three antennas that have the L-band receivers with the new thermal gap assembly (ea02, ea05, and ea26). The red curve represents the average SEFD of the baselines among three other antennas that have EVLA compliant receivers but with the old thermal gap assembly.

sensitivity has resulted around this frequency. Above 1.55 GHz, the sensitivity of the receivers with the new thermal gap assembly has degraded by an average value of ∼3% compared to the receivers with the old thermal gap assembly, again consistent with the lab measurements shown in Figure 1. Our on-the-sky test did not show the sensitivity improvement seen in the lab measurements above 1.95 GHz.

We note that the sensitivity degradation as seen in the SEFD curves of Figure 2 between ∼1.6 and 1.8 GHz is very likely due to the spillover contribution from the undersized 62 inch diameter feed that had to be used on the EVLA antennas. Srikanth, in the Feed Preliminary Design Review (February 2002), presented a number of calculated efficiency and spillover plots, and showed that an optimum feed with a 75 inch diameter would have superior performance. However, such a feed was too big to install on an EVLA antenna without having to remove load-bearing metal in the backup structure. The spillover analysis plot for a 62 inch diameter feed is reproduced here in Figure 4 for elevations of 90, 60 and 30 degrees. It predicts an increase of up to 4 K (∼33%) between 1.6 and 1.8 GHz, consistent with the increase in the SEFD (e.g., the blue curve in Figure 2).

Overall, our results show a net sensitivity improvement at L-band due to the new thermal gap assembly. This should benefit continuum observations which require the full L-band (1–2 GHz) frequency range. Moreover, the clear sensitivity improvement in the lower half of the L-band will be of importance to various spectral line observations such as Galactic and extragalactic HI 21 cm studies (up to redshifts of $z \sim 0.42$ for extragalactic HI), and redshifted OH 18 cm lines ($0.04 \gtrsim z \lesssim 0.72$).

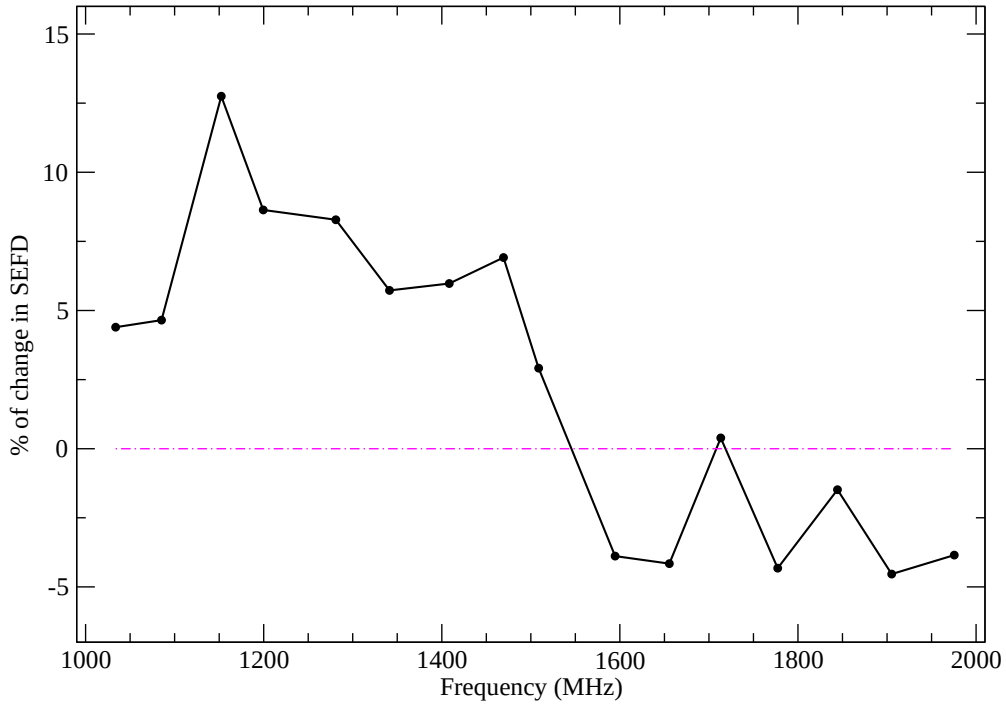

Figure 3: The percentage change in the SEFD due to the new thermal gap assembly relative to the old thermal gap assembly. Positive values reflect lower SEFDs due to the new thermal gap design, and therefore improvement in the sensitivity.

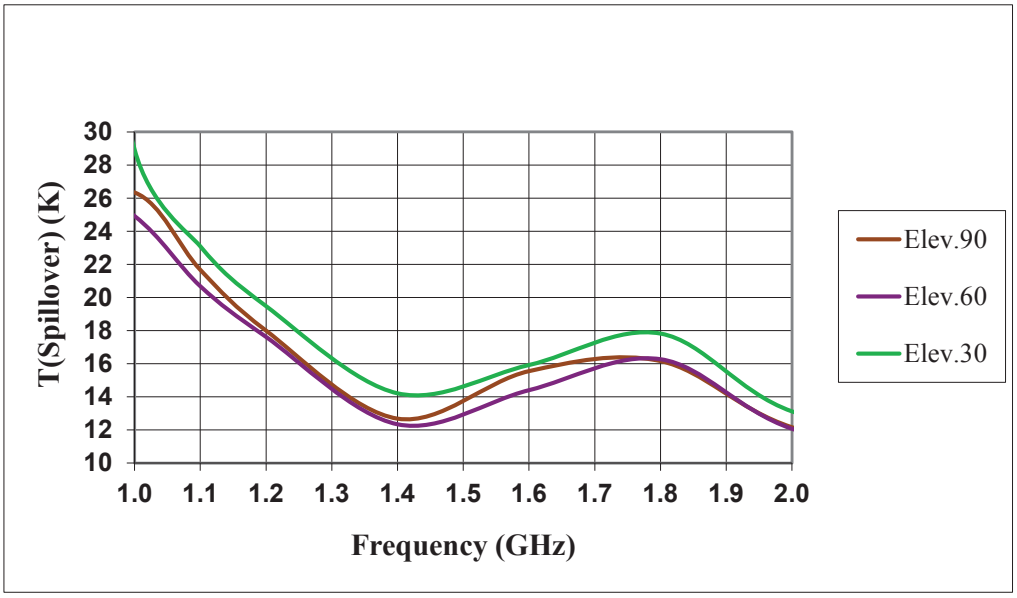

Figure 4: Calculated spillover of the 62 inch diameter L-band feed on an EVLA antenna at elevation angles of 90, 60 and 30 degrees. Adapted from the presentation of S. Srikanth at the Feed Preliminary Design Review (February 2002).

5 Acknowledgements

We would like to thank K. Sowinski and M. Rupen for their help in setting up the test observations, M. Stennes for providing the thermal-gap design for the S-band receiver and H. Dinwiddie who adapted the design for the L- and C-bands, D. Dillon for performing the lab measurements used to compare the old versus new thermal gap performance, and W. Grammer for reviewing the Appendix.

Appendix: The Development of the New Thermal-Gap Assembly of the L- and C-Band Receivers of the EVLA

In the cryogenic receivers built for the EVLA, the thermal isolation between the outside world and the cooled 50 and 15 K stages, where the OMT and low-noise amplifiers are located, is done with a waveguide structure known as a "thermal transition" or "thermal gap". A narrow break of a few thousandths of an inch in the input waveguide is used to separate the 300 K external temperature and the cold stages inside the cryostat. Without it, the critical internal components cannot be cooled adequately, which is vital to achieve the most sensitive radiometers possible.

The design originally used in the L-band receiver had the thermal-gap positioned between the circular-to-square transition and the orthomode transducer (OMT). The feed has a circular waveguide output while the OMT has a square waveguide input, therefore a waveguide adapter is required. Using a thermal-gap with a square cross-section was somewhat unusual as it is harder to provide it with a quarter-wave choke flange to help prevent signal leakage from occurring across the joint. It was based on a legacy design from the early days of the development of an octave bandwidth OMT carried out by P. Lilie, L. Locke and later by G. Coutts. The thermal-gap had essentially been an afterthought while all the creative effort went into getting the novel quadridge OMT design which needed to be wideband, low-loss and free of trapped mode resonances. The use of the early thermal-gap design was retained after the OMT design was successfully completed.

The square aperture thermal-gap did significantly simplify the mechanical design of the input path of the receiver. While easier to manufacture, it had one slight RF problem that was soon discovered. A huge bump in noise temperature occurred at about 1.2 GHz. This was a cavity resonance that arose within the cryostat from leakage in the waveguide path through the gap. It was eliminated by using a strip of AN72 absorber wrapped around the outside circumference of the thermal-gap. While the absorber cured the resonance problem, it also meant a certain amount of noise could leak into the astronomical signal, but it was assumed to be small enough to ignore.

It wasn't until the prototype of the upgraded VLBA C-band receiver was completed in April 2011 that it was realized that there might be significant gains to be made by redesigning the L-band thermal-gap. During the VLBA C-band upgrade project the old VLBA C-band cryostat had to be utilized, which required the fitting of the new EVLA 4–8 GHz OMT into the old cryostat. The biggest problem with this upgrade path was that the new EVLA receiver utilized the larger, Model 350 refrigerator while the old VLBA receiver used the smaller, Model 22 unit. The reduced thermal capacity of the refrigerator could result in the sensitivity of the upgraded receiver being significantly degraded, especially as the old VLBA receiver had its septum polarizer tied to the 50 K stage. Moreover, there was a need to tie the new OMT to the 15 K stage because it has higher resistive loss. This requirement would have thermally loaded the Model 22 fridge further.

Various mechanical engineering attempts were made (by H. Dinwiddie) for the prototype receiver to operate as cold as possible, leading to the conclusion that the simple thermal-gap design that has been used in the EVLA C-band receiver, which itself was based on the earlier L-band design, would need to be improved.

The new design, which placed the gap in the circular waveguide section, made it possible to use longer insulating fiberglass standoffs that reduced the thermal loading on the 15 K stage. This reduced the operating temperature down into the acceptable 12–18 K range. More importantly, the new choke flange used in the thermal gap also improved the sensitivity of the receiver. Compared to the EVLA C-band receiver, the receiver temperature dropped by nearly 5 K at the low-end of the band and by 2–3 K at the high-end. With this change, the VLBA C-band upgraded prototype had a receiver temperature that was less than 10 K over 95% of its frequency range (i.e., 4.2–8.0 GHz). This receiver was also much superior to the EVLA receiver, prompting the need to retrofit all the EVLA C-band receivers with the new thermal gap design.

The success of the new thermal-gap in the C-band system led to redesigning the unit used in the EVLA L-band receiver. With its location higher up in the circular waveguide path, it also allowed the cavity resonance absorbing strip to be eliminated. The new design was scaled in frequency from the thermal-gap that M. Stennes had developed for the EVLA S-band receiver several years earlier and was adapted for use in both the EVLA L- and C-band receivers by H. Dinwiddie.